Sensitivity analysis on the effect of key parameters on the performance of parabolic trough solar collectors

# Sensitivity analysis on the effect of key parameters on the performance of parabolic trough solar collectors

**Luis S. W. Muhlen[1], Behzad Najafi[2], Fabio Rinaldi[2*], Renzo Marchesi[2]**

[1]Scuola di Ingegneria Industriale, Politecnico di Milano, Campus di Piacenza, Via Scalabrini, 76, 29100 Piacenza, Italy
[2] Dipartimento di Energia, Politecnico di Milano, Via Lambruschini, 4, 20156, Milano, Italy

Email: fabio.rinaldi@polimi.it

**Abstract**. Solar troughs are amongst the most commonly used technologies for collecting solar thermal energy and any attempt to increase the performance of these systems is welcomed. In the present study a parabolic solar trough is simulated using a one dimensional finite element model in which the energy balances for the fluid, the absorber and the envelope in each element are performed. The developed model is then validated using the available experimental data. A sensitivity analysis is performed in the next step in order to study the effect of changing the type of the working fluid and the corresponding Reynolds number on the overall performance of the system. The potential improvement due to the addition of a shield on the upper half of the annulus and enhancing the convection coefficient of the heat transfer fluid is also studied.

## 1. Introduction

Energy sources that are considered sustainable have become increasingly popular and sought after with the ever growing general concern for the negative effects of human interference in the environment [1-2] and many studies have also been carried out in order to optimize the devices to enhance the efficiency of utilization of such resources [3]. Amongst the technologies being developed in the attempt to control and reverse the current dependency on dangerous and polluting energy sources, the direct use of solar radiation to generate heat has been a successful and widely applicable form of replacing the use of fossil fuels from very small scale installations to large power plants.

The present project intends to study the optimization of the parameters of one of the most used configurations for large scale solar plants: the parabolic trough. At the cost of only being able to reach lower temperatures, restricted at around 550°C for current technologies, this configuration is a promising option in the case of macro scale power generation since several modules can be installed one after the other, allowing the creation of very large plants. The parabolic trough solar system with evacuated receivers is the most economically promising macro scale solar generation available technology today [4].

Studies have been developed for several specific finalities. For chemical plants, it is often desired to reach higher fluid temperatures, while for steam generation the maximum temperature isn't as relevant, allowing the use of cheaper technologies. For electricity generation through the use of steam,

---

*Corresponding author

it becomes very important to achieve high efficiency rates in order to decrease the plant size. A combined solar plant for electricity generation has been presented by Manzolini et al [5], using saturated steam as a low temperature fluid, and then a synthetic oil for super-heating. The use of molten salts is an alternative to try to improve even more the efficiency of the plant, through the use of higher temperatures. A solar plant for industrial purposes was presented by Manzolini et al [6]. Structural parameters were evaluated by Giannuzzi et al [7]. Studies on existing solar plants and their applicability on specific locations have been performed in [8-10] and several analytical correlations have been studied and developed for the parabolic trough solar concentrator. In order to evaluate thermal losses and optimize power plant systems, different 1D to 3D models have been developed [4][11][12-15]. Economic optimizations and analysis have been performed for real case scenarios as well as for hypothetical situations [8][16-18]. Studies on specific improvements on the general layout of the trough collector have been made to provide alternative methods for improving overall efficiency, such as the possibility of using fins inside the collecting tube to promote homogenization of the fluid [19], using capillary tubes to improve the wet surface and reduce the effect of the dual phase condition that may occur at low flow rates [20] or using a thermal isolating material covering the upper half of the tube, where there is no focused light incidence, to reduce radiation losses and reduce natural convection [21].

In the present work, a 1D (axial) analytical approach for simulating the fluid flow and the heat exchange in the collector tube was employed. After validating the developed model using experimental data, the simulations were performed utilizing different working fluids. The effect of geometric parameters was next investigated by analyzing the effect of Reynolds number in the efficiency. Afterwards, the effect of adding a shield on the upper half of the annulus was analyzed where the simulations are performed both for vacuum and atmospheric pressure conditions. Finally, the effect of the strategies leading to an enhancement on the convection coefficient of the heat transfer fluid, as suggested in the literature, was studied and the corresponding simulation were carried out employing both oil and the molten salt as heat transfer fluids.

## 2. Model Description

The implemented model is largely based on the model proposed by Padilla et al [12]. It is a 1D model that simulates the heat transfer between four elements of the solar collector: the heat transfer fluid (HTF), the absorber tube, the glass envelope and the structural brackets, along with the thermal losses to the environment and the incident solar energy. The total length of the solar collector is divided into elements in which the temperatures and all other properties are considered to be constant.

The absorber and the glass envelope are circular coaxial tubes with constant dimensions across the length of the model. The thermal conductivity of the absorber is assumed to be homogeneous and independent of temperature for the temperature range of the through. It is covered by a thin layer of a coating material with enhanced irradiative heat transfer properties with no effect to the other forms of heat transfer. The HTF properties are functions of temperature, but not pressure. The flow is considered to be turbulent and fully developed for the entire length of the trough. No phase change is simulated, therefore the model doesn't accept saturated vapor as HTF. For the envelope, no radial temperature gradient is considered, only axial. It is considered to have a non-null absorption coefficient, therefore it absorbs part of the solar irradiation. It maintains a controlled atmosphere in the annulus between the absorber and the envelope that can be simulated as a vacuum with any chosen pressure, or even atmospheric pressure to determine the system properties when there is a leakage. The brackets are considered to be fins equally spread along the length of the absorber, with intervals multiple of the adopted mesh size.

Only the following heat transfer mechanisms are assumed to exist: forced convection between the absorber and the HTF, conduction along the width of the absorber, radiation and natural convection between the absorber and the glass envelope, conduction between the absorber and the brackets, natural or forced convection between the envelope and the atmospheric air, radiation between the absorber and the sky and, finally, radiation between the Sun and the absorber and envelope. The model

doesn't simulate radiation losses from the absorber to the environment or the sky, as the envelope is assumed to be opaque to the radiation emitted by the coating surface. A representation of the model using the thermal resistances is demonstrated in figure 1.

The model only simulates the steady state condition. Although each section of the mesh can have different temperatures for the envelope and the absorber, the net heat exchange between one section and its neighboring sections is null, condition that is only true if the temperature gradients are constant along the length of the collector. From these assumptions, an energy balance for each section dictates that the sum of all the heat exchanged is null for both the envelope and the absorber.
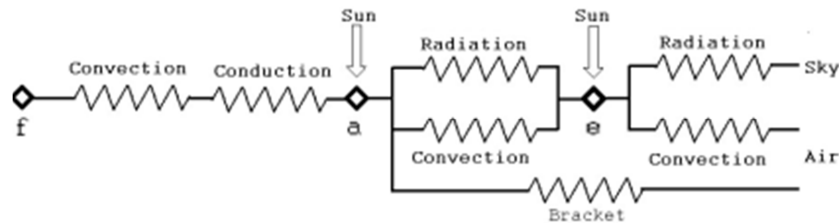


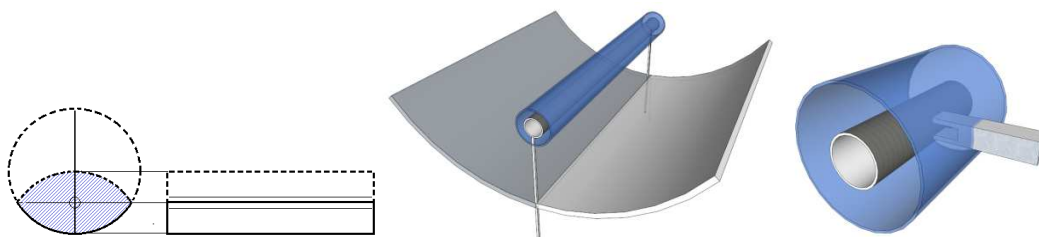**Figure 1.** Representation of the model through the use of thermal resistances [9]



**Figure 2.** Representation of the modeled mirror

*1.1. Convection and conduction between the absorber and the HTF*

The convective and conductive heat transfer is determined by:

$$\dot{Q}_{a \to f} = \frac{T_a - T_f}{\frac{1}{\pi \cdot Nu_D \cdot k_f} + \frac{\ln(D_{a,o}/D_{a,i})}{2 \cdot \pi \cdot k_a}} \tag{1}$$

Where the Nusselt number is calculated by the relation given by Gnielinski, with the correction factor recommended by Petukhov and Roizen [22]:

$$Nu_D = \frac{\frac{C_f}{2} \cdot (Re_D - 1000) \cdot Pr}{1 + 12.7 \cdot (\frac{C_f}{2})^{0.5} \cdot (Pr^{2/3} - 1)} \cdot \left(\frac{Pr}{Pr_w}\right)^{0.11} \tag{2}$$

The friction coefficient is obtained using the Filonenko correlation [23]:

$$C_f = (1.58 \cdot \ln(Re_D) - 3.28)^{-2} \tag{3}$$

*1.2. Natural convection between the absorber and the envelope*

Two distinct cases were implemented for the natural convection in the annulus, one assuming vacuum and other assuming normal pressures. A vacuum was considered for pressures below 1 Torr, although the recommendation is to use a pressure as low as 0.0001 Torr to reach the free molecule regime that greatly reduces the heat transfer. In the vacuum case, the natural convection heat transfer is given by:

$$\dot{Q}_{a\rightarrow e,conv} = h_{a\rightarrow e} \cdot \pi \cdot D_{a,o} \cdot (T_a - T_b) \tag{4}$$

Assuming a thermal accommodation coefficient equal to 1, as it is recommended for most solid – gas interactions, the convective heat transfer coefficient is given by [24]:

$$h_{a\rightarrow e} = \frac{k_g}{\frac{D_{a,o}}{2}\cdot \ln(\frac{D_{e,i}}{D_{a,o}}) + \frac{\lambda\cdot(9\cdot\gamma-5)}{2\cdot(\gamma+1)}\cdot(\frac{D_{e,i}}{D_{a,o}}+1)} \tag{5}$$

$$\lambda = 2.331 \cdot 10^{-20} \cdot \frac{(T_a + T_e)}{2} \cdot \frac{1}{P_{an}\cdot D_{mol}^2} \tag{6}$$

For air, the molecular diameter $D_{mol}$ equals 3.66 x 10-8 cm. While normally the thermal conductivity of the annulus gas is assumed to be only a function of the temperature, in a vacuum scenario it is assumed to be directly proportional to the pressure up to the 1 Torr mark.

In the case where normal pressures are used for the annulus, the following correlation given by Kuehn and Goldstein is used to determine the Nusselt number in the annulus [25]:

$$Nu_D = (Nu_{D,cond}^{15} + Nu_{D,conv}^{15})^{1/15} \tag{7}$$

$$Nu_{D,cond} = \frac{2}{\ln(D_{e,i}/D_{a,o})} \tag{8}$$

$$Nu_{D,conv} = \frac{2}{\ln(\frac{1+6.659\cdot Ra^{-0.294}}{1-2.441(Ra\cdot(D_{e,i}/D_{a,o})^3)^{-0.206}})} \tag{9}$$

### 1.3. Radiation between the absorber and the envelope

All surfaces are assumed to be gray and opaque. Each section of the grid is considered to be closed on the side by adiabatic walls that reflect but do not emit radiation. The view factors [26] are given by:

$$F_{e\rightarrow a} = \frac{1}{R} - \frac{1}{\pi\cdot R}[acos(\frac{B}{A}) - \psi\cdot acos(\frac{B}{R\cdot A}) - \frac{B}{2\cdot L}\cdot asin(\frac{1}{R}) + \frac{\pi\cdot A}{4\cdot L}] \tag{10}$$

$$F_{e\rightarrow e} = 1 - \frac{1}{R} + \frac{2}{pi\cdot R}\cdot atan(\frac{2\cdot\sqrt{R^2-1}}{L}) - \frac{L}{2\pi\cdot R}\cdot[\chi\cdot asin(\varphi) - asin(\frac{R^2-2}{R^2}) + \frac{\pi}{2}(\chi - 1)] \tag{11}$$

Where:

$$\psi = \frac{\sqrt{(A+2)^2 - (2\cdot R)^2}}{2\cdot L} \tag{12}$$

$$\chi = \frac{\sqrt{4R^2 + L^2}}{L} \tag{13}$$

$$\varphi = \frac{4(R^2-1) + L^2/R^2(R^2-2)}{L^2 + 4(R^2-1)} \tag{14}$$

$$R = \frac{D_{e,i}}{D_{a,o}} \tag{15}$$

$$L = \frac{h}{D_{a,o}} \tag{16}$$

$$A = L^2 + R^2 - 1 \tag{17}$$

$$B = L^2 - R^2 + 1 \tag{18}$$

The view factor $F_{a\rightarrow e}$ is found using symmetry and the view factors for the side walls are found using the property that the sum of all view factors for one surface equals one. Assuming that both side walls are a single surface:

$$F_{a\rightarrow e} = F_{e\rightarrow a} \frac{D_{e,i}^2}{D_{a,o}^2} \tag{19}$$

$$F_{a\rightarrow s} = 1 - F_{a\rightarrow e} \tag{20}$$

$$F_{e\rightarrow s} = 1 - F_{e\rightarrow e} - F_{e\rightarrow a} \tag{21}$$

The thermal resistances and the heat transfers are given by:

$$R_{a \to e} = \frac{(1-\varepsilon_a)}{\varepsilon_a \cdot A_a} + \frac{(1-\varepsilon_e)}{\varepsilon_e \cdot A_e} + \frac{1}{A_a \cdot F_{a \to e} + ((A_a \cdot F_{a \to s})^{-1} + (A_e \cdot F_{e \to s})^{-1})^{-1}} \qquad (22)$$

$$\dot{Q}_{a \to e, rad} = \sigma \frac{(T_a^4 - T_e^4)}{R_{a \to e}} \qquad (23)$$

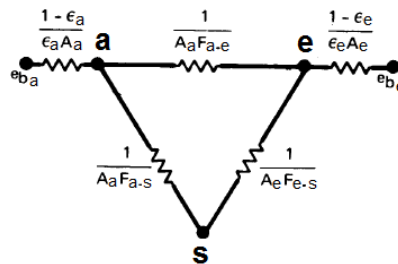The Thermal resistance given in equation 22 can be elaborated using Oppenheim circuit shown below



**Figure 3**. Oppenheim Circuit.

### 1.4. Conduction through the support brackets

    The support brackets are modeled as fins made of carbon steel, composed by two segments with different cross sections. In the first segment, connected to the base of the solar receiver, the cross section is a pair of rectangular plates with dimensions 25.4 x 3.175 mm and 25.4 mm length. The second segment is the support tubes, with cross section formed by a pair of hollow squares with 25.4 mm sides and 3.175 mm thickness. Since the second segment covers most of the length, it is considered to have a length equal to the focal distance of the mirror.

    Due to the length of the brackets, an infinite length fin model is used [27]. The temperature at the intersection is given by:

$$\frac{\theta_a}{\theta_b} = \frac{1}{\cosh(m_{b,1} \cdot L_{b,1}) + \frac{\zeta_{b,2}}{\zeta_{b,1}} \cdot \sinh(m_{b,1} \cdot L_{b,1})} \qquad (24)$$

And the heat loss through the brackets is given by:

$$\dot{Q}_b = \frac{2 \cdot \zeta_{b,1} \cdot (T_a - T_{air}) \cdot \cosh(m_{b,1} \cdot L_{b,1}) - \frac{\theta_a}{\theta_b}}{\sinh(m_{b,1} \cdot L_{b,1})} \qquad (25)$$

Where:

$$m_{b,1} = \sqrt{\frac{h_b \cdot Per_1}{k_b \cdot Ac_1}} \qquad (26)$$

$$\zeta_{b,j} = \sqrt{h_b \cdot Per_j \cdot k_b \cdot Ac_j} \text{ for } j = 1,2. \qquad (27)$$

    The worst case scenario was adopted to determine the convective coefficient: forced convection with a square orientation instead of a diamond orientation.

$$Nu_b = 0.14 \cdot Re_b^{0.666} \qquad (28)$$

### 1.5. Convection between the envelope and the atmospheric air

    For forced convection, the following correlation was used to determine the Nusselt number:

$$Nu_D = (1 + (\frac{Re_D}{282000})^{\frac{5}{8}})^{\frac{4}{5}} \cdot 0.62 \frac{Re_D^{0.5} \cdot Pr_{film}^{1/3}}{(1 + (\frac{0.4}{Pr_{film}})^{\frac{2}{3}})^{\frac{1}{4}}} + 0.3 \qquad (29)$$

The heat loss through convection is then calculated as follows:

$$\dot{Q}_{e \to air,conv} = Nu_D \cdot k_{film} \cdot \pi \cdot (T_e - T_{air}) \tag{30}$$

### 1.6. Radiation losses from the envelope to the sky

For this analysis several simplifications were made. The sky is considered to be a black body with constant temperature, function of the air temperature. The envelope views only the sky and the mirror, and with the exception of the sides, half of the surface is covered by sky and half by mirror. To calculate the views of the sides, the absorber is placed in the focal distance of the mirror, which is half of the radius of the mirror's circumference, as represented on figure 2.

An average radius is calculated from these assumptions, which is then used to model the sides as circles with the same area. This average radius is given by:

$$\bar{r} = 2\frac{\sqrt{3}}{3\pi} \cdot D_m \cdot atanh(\sqrt{3} \cdot \tan(\tfrac{\pi}{8})) - \frac{D_{e,o}}{2} \tag{31}$$

Then the view factor of the sides, which is a function of the position x of the segment being analyzed in relation to the edges of the trough, is given by:

$$F_{e \to s} = \frac{atan(\bar{r}/x) + atan(\bar{r}/(L-x))}{\pi} \tag{32}$$

Finally, the view factor for the sky is:

$$F_{e \to sky} = \frac{(1 - F_{e \to s})}{2} \tag{33}$$

The heat loss through radiation to the sky is taken from equations given by Padilla et al [12] while the sky temperature is found using the relation given by Swinbank [28]. The Sun light that reaches the mirror is reflected back to the absorber. A series of corrective factors are used to represent the losses due to part of the light reaching the collector not reaching the absorber, as seen in table 1 [12]:

**Table 1.** Mirror losses coefficients.

| | | |
|---|---|---|
| Heat collection element shadowing ($\gamma 1$) | Luz black chrome | 0.974 |
| | Luz cermet | 0.971 |
| Twisting and tracking error ($\gamma 2$) | | 0.994 |
| Geometry accuracy of the collector mirrors ($\gamma 3$) | | 0.980 |
| Mirror clearness ($\gamma 4$) | | 0.950 |
| Dirt on heat collection element ($\gamma 5$) | | 0.980 |
| Miscellaneous factor ($\gamma 6$) | | 0.960 |
| Clean mirror reflectivity | | 0.935 |

The total heat from the Sun absorbed by the absorber and by the envelope is:

$$\dot{Q}_{sun \to a} = \gamma \cdot \tau_e \cdot \alpha_a \cdot 1.01 \cdot I_{bn} \cdot \frac{D_m}{2} \cdot \sqrt{3} \tag{34}$$

$$\dot{Q}_{sun \to e} = \gamma \cdot \alpha_e \cdot 1.01 \cdot I_{bn} \cdot \frac{D_m}{2} \cdot \sqrt{3} \tag{35}$$

Where the term $\gamma$ is the product of all the terms in table 1. The factor 1.01 is added in the equation to make up for internal reflections in the trough [29]. The solar radiation is considered to reach the trough perpendicularly and geometrical end losses of the collector are not assumed to exist.

The efficiency is calculated as the ratio between the total enthalpy gain (including the gain in kinetic energy) and the total solar energy irradiated on the collector mirror.

### 3. Numerical solution

The energy balance is performed in the HTF, in the absorber and in the envelope. From the simplifications stated before (steady state and no heat transfer in the axial direction for the absorber and the envelope), the energy balance for the HTF gives an equation that is a function of the temperature of the HTF in the previous section and of the temperatures of the HTF and the absorber in the given section. The balance for the envelope gives an equation that is function only of the temperatures of the absorber and the envelope in the given section, and the balance for the absorber returns an equation that is function of the temperatures of the HTF, the absorber and the envelope in the given section:

Absorber balance
$$\frac{Q_a}{G_{Sun}} - \frac{Q_a}{f_{conv}} - \frac{Q_a}{e_{conv}} - \frac{Q_a}{e_{rad}} - Q_{brack_{cond}} = 0 \tag{36}$$

Envelope balance
$$\frac{Q_e}{rad_{Sun}} + \frac{Q_a}{conv_e} + \frac{Q_a}{rad_e} + \frac{Q_a}{rad_e} - \frac{Q_a}{conv_{air}} - \frac{Q_{ae}}{rad_{sky}} = 0 \tag{37}$$

HTF balance
$$\gamma(T_{m1} - T) + AF_{conv}h - m_f(v_f^2 - v_{f_{m1}}^2) = 0 \tag{38}$$

For each element, a guess is made for the temperature of the absorber. From this initial guess, the fluid and the envelope temperatures are found using a golden ratio increment line search, using the energy balance for the fluid and the envelope, respectively. Then the guess for the temperature of the absorber is checked using the energy balance of the absorber and all the temperatures found previously. Using again a line search with golden ratio increments, this procedure is repeated until a temperature is found for the absorber that respects its energy balance. A temperature for the HFC at the start of the trough is required as a boundary condition.

### 4. Model Validation

The model results are validated using the data provided by the Sandia National Laboratory [30], an extensive experimental study performed with a single module from a trough power plant. The available data include Steady State condition final temperatures for the HTF, overall efficiency and heat loss for different HTF flows and initial temperatures, as well as different solar incidences. Tests were also performed with vacuum and with air at ambient pressure in the annulus, and without the glass envelope. The measured data considering the vacuum in the annulus is given in Table 2 and the corresponding validation results are demonstrated in Figure 4.

**Table 2.** Measured data, vacuum in the annulus.

| Test | Direct Normal Irradiation [W/m²] | Wind Speed [m/s] | Air Temperature [ºC] | Inlet Temp. [ºC] | Outlet Temp. [ºC] | Flow Rate [L/min] |
|------|------|------|------|------|------|------|
| **1** | 933.7 | 2.6 | 21.2 | 102.2 | 124.0 | 47.7 |
| **2** | 968.2 | 3.7 | 22.4 | 151.0 | 173.3 | 47.8 |
| **3** | 982.3 | 2.5 | 24.3 | 197.5 | 219.5 | 49.1 |
| **4** | 909.5 | 3.3 | 26.2 | 250.7 | 269.4 | 54.7 |
| **5** | 937.9 | 1.0 | 28.8 | 297.8 | 316.9 | 55.5 |
| **6** | 880.6 | 2.9 | 27.5 | 299.0 | 317.2 | 55.6 |
| **7** | 920.9 | 2.6 | 29.5 | 379.5 | 398.0 | 56.8 |
| **8** | 903.2 | 4.2 | 31.1 | 355.9 | 374.0 | 56.3 |

Tests with two different coatings for the absorber are available. Most of the experiments were done using Syltherm 800 as the HTF, and its thermal properties were obtained from its catalogue [31]. The results obtained were overall close to the measured data, with a difference of 2 to 3 [ºC]. Such errors could be a consequence of imprecise values for the mirror efficiencies and are considered to be within

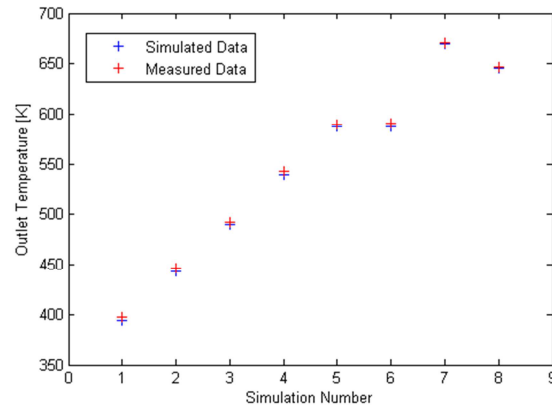acceptable range. It should be mentioned that 2~3°C corresponds to 10~15% in terms of overall energy gain.



**Figure 4** Validation results, vacuum in the annulus.

### 5.  Results and discussions

The results show that, for the utilized model, the temperatures of the HTF and the absorber increase very close to linearly throughout the length of the trough. The temperature of the envelope is almost constant, with a decrease near the ends due to the increase of the ratio of sky and collector viewed by the envelope at the extremities. This happens because the model sees the sides of the collector as sky. In reality, part of this section of the views would be landscape, with a higher temperature than the sky, so the model over estimates those heat losses, even though it is a very subtle overestimation. From these results, the hypothesis that the net heat flux is zero across the length of the absorber and the envelope is acceptable.

The simulations with vacuum at low pressures, around 10-4 Torr, show that the heat losses from the absorber to the envelope are negligible, and most of the solar energy absorbed by the coating surface is transferred to the HTF. The losses to the environment come mostly from the energy absorbed by the envelope. The most important factor that reduces the overall efficiency of the trough is the inefficiencies of the mirror, which this model simplifies as constant factors that multiply the incident solar energy. When the vacuum is broken, the thermal losses from the absorber increase slightly. Conditions that reduce the convective heat transfer coefficient for the HTF can greatly increase the temperature of the absorber, making the thermal losses more relevant. The losses through the support brackets are the highest for most of the simulations made.

The parameters of the considered case study are presented in table 3. As it was expected, higher HTF temperatures increase the losses and decrease the efficiency of the trough. This must be considered when evaluating the benefits of an increased temperature in the overall efficiency of the plant. The temperature distribution of the HTF along the collector length for the case study is shown in Figure 5. The breakdown of the thermal losses in two pressure case is given in table 4.

**Table 3** Parameters for example simulations.

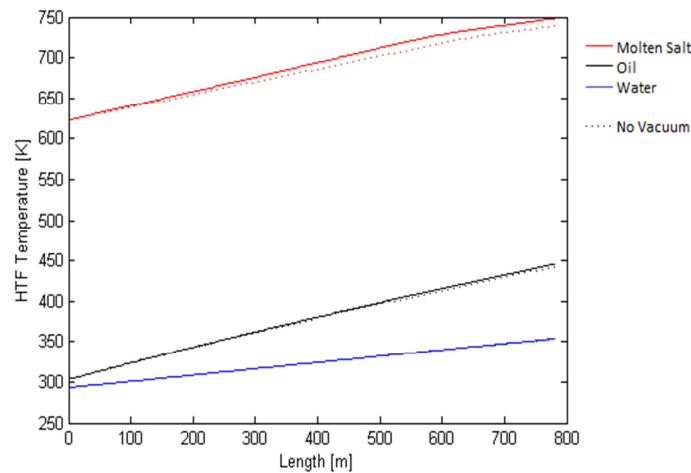| | |
|---|---|
| Direct Normal Irradiation | 900 W/m2 |
| Mass Flow | 10 kg/s |
| Air Velocity | 2.6 m/s |
| Air Temperature | 20 ºC |
| Trough Length | 780 m |
| Mirror Aperture | 5 m |
| Bracket Separation | 3.9 m |
| $D_{a,i}$ | 0.06 m |
| $D_{e,i}$ | 0.1 m |

**Figure 5**. Temperature distribution of HTF along the collector length for different fluids.

**Table 4.** Break down of thermal losses

| Annulus Pressure | Vacuum | atmospheric |
|---|---|---|
| $Q_{b_{cond}}$ (w) | $7.284. \, 10^3$ | $7.158. \, 10^3$ |
| $Q_{a-env_{conv}}$ (w) | $0.0810$ | $2.973. \, 10^5$ |
| $Q_{a-env_{rad}}$ (w) | $2.994.10^4$ | $2.778.10^4$ |
| $Q_{air_{conv}}$ (w) | $6.4822 \,.10^4$ | $2.741. \, 10^5$ |
| $Q_{sky_{rad}}$ (w) | $2.957.10^4$ | $1.154. \, 10^5$ |

A sensitivity analysis was performed in order to investigate the effect of the Reynolds number (as a function of both the absorber diameter and the mass flow rate) to the overall efficiency of the trough. Varying the internal absorber diameter from 20 to 100 mm and varying the mass flow from 2 to 34 kg/s, the efficiencies were simulated for both oil and molten salt as the HTF. The results indicate that there is a minimum tolerable mass flow rate that, below which, the efficiency drops to unacceptable levels. This threshold isn't reached in this simulation for the oil, but was present for the molten salt, indicating that when using it as a HTF, especial precautions need to be taken when dimensioning the mass flow rate. Figure 6 shows the efficiency curves as a function of the Reynolds number, for several absorber diameters where oil is used as the HTF.

To simulate the potential improvement due to the addition of a shield on the upper half of the annulus as proposed by Al-Ansary [21], the calculations for the absorption of solar radiation, for the convective losses to the environment and for the radiation losses to the sky were changed. The total mirror aperture was reduced by the value of the envelope diameter, the view factor from the envelope to the sky was reduced to zero and the convection losses were reduced by 25%. These changes simulate the covering of the upper half of the envelope with an isolating, opaque material, which drastically reduces the losses to the environment, but also reduces the amount of incoming solar energy slightly. This change does not simulate the reduction in the natural convection inside the annulus that should also be a benefit of the method proposed. It is expected that the benefit of such a method will vary depending on the losses to the environment, so this analysis was performed for the annulus pressure varying from vacuum to atmospheric pressure, and the adopted working fluid was molten salt, due to the higher operating temperature. The effect of application of shield for different

annulus pressures is demonstrated in Figure 7. The HTF temperature profile along the collector in which the shield is used is simulated in Figure 8
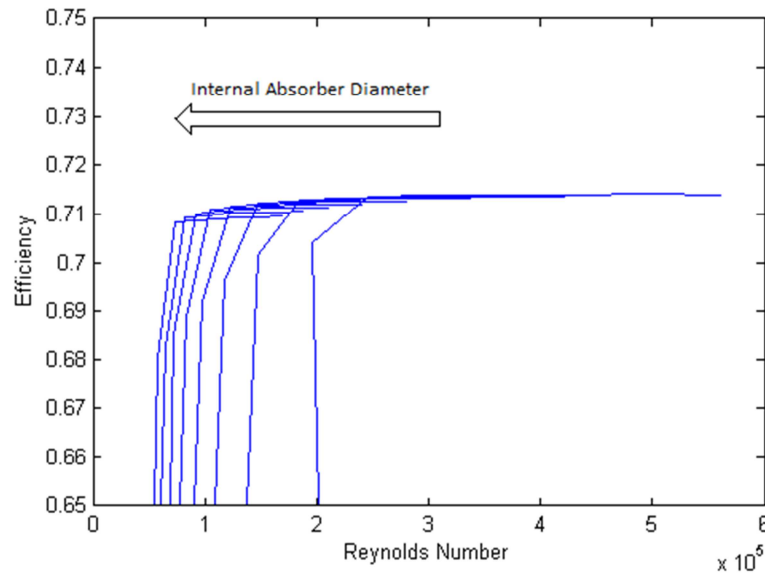


**Figure 6.** Efficiency curves as a function of the Reynolds number, for several absorber diameters, using molten salt as HTF.

The results indicate that the reduction of the thermal losses doesn't compensate for the reduction of the solar gains. For atmospheric annulus pressure the method gets close to being advantageous, indicating that in a scenario where the losses were much more relevant, this could be a promising technique.
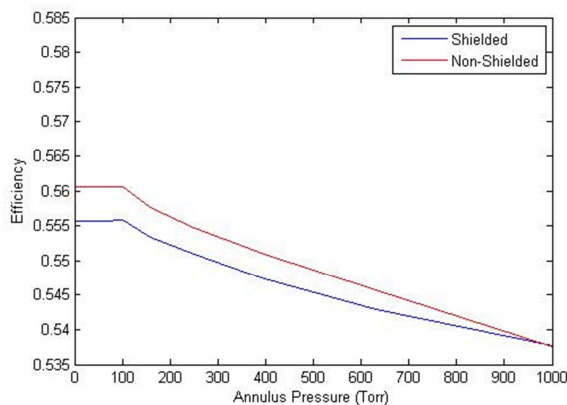


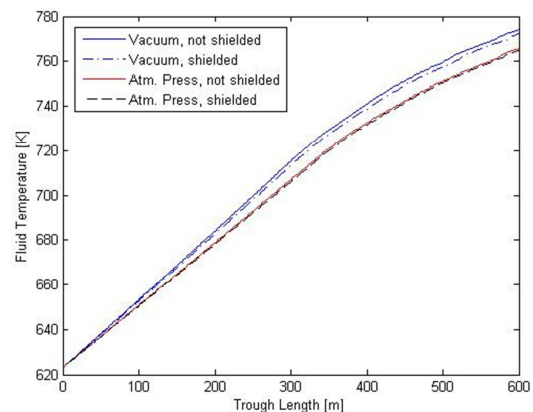**Figure 7.** Shield simulation – Efficiency as a function of the annulus pressure.

**Figure 8.** Shield simulation – HTF temperature along the length of the collector.

Studies suggest methods to boost the efficiency of the trough by increasing the convection coefficient of the HTF [19-20]. To simulate these gains and other possible techniques, a static parameter was added, increasing the convection artificially. Simulations were made with increases of up to 200% for the convection coefficient for standard trough collectors using molten salt and synthetic oil as the HTF. Definition of convection coefficient modifier $c_{h_f}$ which is multiplied by the

Nu number can be represented in the following equation which is expressing the convective and conductive heat transfer between the absorber and the fluid.

$$Q_{a-f_{conv}} = \frac{(T_a - T)}{\dfrac{1}{\pi Nu_f k_f c_{h_f}}} + \log\left(\frac{Da_{out}}{2Da_{in}} \cdot \frac{k_a}{\pi}\right) \tag{39}$$

This analysis was made simulating a 600 m long trough with a mirror opening of 5 m, mass flow of 6 kg/s and an internal absorber diameter of 0.04 m. Initial temperature for the oil was 30 °C, and for the molten salt it was 350 °C. The effect fluid convection modifier factor on the total efficacy is demonstrated in Figure 9.

The simulations indicate that the efficiencies for the scenario with oil as HTF are almost unaffected by the increase in the convection coefficient. This is most likely due to the smaller thermal losses present in reason of the lower operating temperature, as well as the smaller dependency of the efficiency with the Reynolds number that was described above for this range of diameter and mass flow. On the other hand, the efficiencies were increased considerably for the molten salt scenarios.
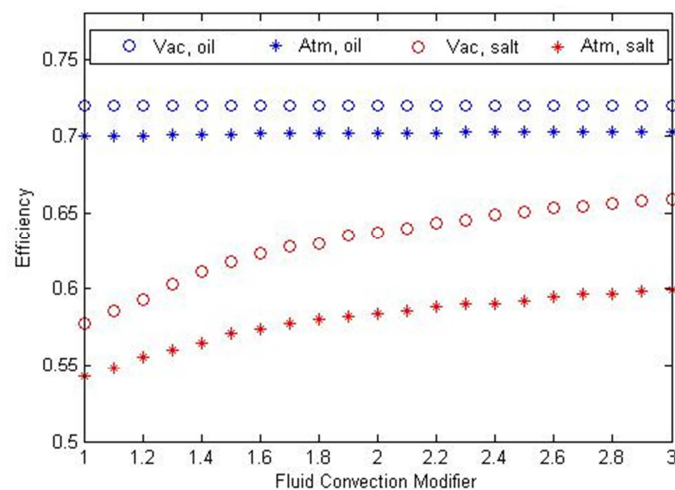


Figure 9. Efficiency as a function of the fluid convection modifier factor.

## 6. Conclusion

A one-dimensional model for simulating the heat transfers between the heat transfer fluid, absorber and envelope of a solar trough collector and the environment was implemented and the developed model was next validated using the available experimental data. In the next step, simulations were performed for different working fluids and the corresponding temperature profiles were obtained. Sensitivity analysis on the effect of the Reynolds number on the performance of the systems was next carried out and a diagram demonstrating the efficiency curves as a function of the Reynolds number for different internal absorber diameter was provided. Afterwards the effect of adding a shield on the upper half of the annulus, as suggested in the literature, was performed and it was demonstrated that the mentioned strategy can only be advantageous at very high pressures. Finally the effect of enhancing the convection coefficient of the heat transfer fluid was investigated and it was demonstrated that increasing the convection coefficient in case of the oil has a negligible effect while it can considerably increase the efficiency in case of the molten salt. It is noteworthy that since in the this study the analysis on the parameters affecting the  losses associated with the mirror and its optical inefficiencies was not performed, an upgrade to the present work is to include a more precise formulation of the mirror parameters and to analyze the corresponding affecting parameters.

## Nomenclature

| | | | |
|---|---|---|---|
| A | Surface area [m²] | Ra | Rayleigh number |
| Ac | Cross section area [m²] | Re | Reynolds number |
| Cf | Friction coefficient | T | Temperature [K] |
| D | Diameter [m] | V | Velocity [m/s] |
| F | View factor | x | Distance in the axial direction [m] |
| h | Convective heat transfer coefficient [W/m².K], | | |
| h | Mesh size [m] | **Greek symbols** | |
| I | Solar irradiance [W/m²] | α | Absorptance |
| k | Thermal conductivity [W/m.K] | γ | Ratio of specific heats |
| L | Total length [m] | ε | Emissivity |
| $\dot{m}$ | Mass flow rate [kg/s] | σ | Stefan Boltzmann constant |
| Nu | Nusselt number | θ | Temperature difference with the environment [K] |
| P | Pressure [Torr] | | |
| Per | Perimeter [m] | τ | Transmittance |
| Pr | Prandtl number | | |
| $\dot{Q}$ | Heat transfer flux per trough unit length [W/m] | | |
| r | Radius [m] | | |
| R | Thermal resistance | | |

## Subscripts

| | | | |
|---|---|---|---|
| 1 | Section 1 | e | Envelope |
| 2 | Section 2 | film | Film |
| a | Absorber | f | Fluid |
| an | Annulus | i | Internal, i-th section |
| b | Bracket | m | Mirror |
| air | Air | mol | Molecular |
| bn | Normal beam | o | Outer |
| cond | Conduction | s | Perpendicular section, side |
| conv | Convection | w | Wall |

## References

[1] Shirazi A, Aminyavari M, Najafi B, Rinaldi F, Razaghi M 2012, Thermal–economic–environmental analysis and multi-objective optimization of an internal-reforming solid oxide fuel cell–gas turbine hybrid system. Int J Hydrogen Energy 37 19111-24.

[2] Zago M, Casalegno A, Marchesi R, Rinaldi F 2011, Efficiency Analysis of Independent and centralized heating systems for residential buildings in northern Italy, Energies **4** – Special Issue Energy Efficient Building Design 2115-2131.

[3] Selleri T, Najafi B, Rinaldi F, Colombo G. 2013, Mathematical Modeling and Multi-Objective Optimization of a Mini-Channel Heat Exchanger Via Genetic Algorithm. ASME J. Therm. Sci. Eng. Appl. **5** (3) , art. no. 031013;DOI: http://dx.doi.org/10.1115/1.4023893.

[4] Gong G, Huang X, Wang J and Hao M 2010, An optimized model and test of the China's first high temperature parabolic trough solar receiver, *Solar Energy* **84** 2230–2245

[5] Manzolini G, Giostri A, Saccilotto C Silva P and Macchi E 2011 Development of an innovative code for the design of thermodynamic solar power plants part B: Performance assessment of commercial and innovative technologies, *Renewable Energy* **36** 1993-2003

[6] Manzolini G, Bellarmino M, Macchi E and Silva P 2011, Solar thermodynamic plants for cogenerative industrial applications in southern Europe, Rene. Energy **36** 235-243

[7] Giannuzzi G M, Majorana C E, Miliozzi A, Salomoni V A, Nicolini D 2007 Structural Design Criteria for Steel Components of Parabolic-Trough Solar Concentrators , *Trans. of the ASME 382 / Vol. 129*

[8] Poullikkas A 2009 A Economic analysis of power generation from parabolic trough solar thermal plants for the Mediterranean region—A case study for the island of Cyprus, *Rene Sust. Energy Rev.* **13** 2474–2484

[9] García A F, Zarza E,Valenzuela L andPérez M 2010 Parabolic-trough solar collectors and their applications, *Rene Sust. Energy Rev.* **14** 1695–1721

[10] O.Badran O and Eck M  2006The application of parabolic trough technology under Jordanian climate, *Rene. Energy* **31** 791–802

 [11]  Manzolini G, Giostri A, Saccilotto C, Silva P and Macchi E 2011 Development of an innovative code for the design of thermodynamic solar power plants part A: Code description and test case, *Rene. Energy* **36** 1993-2003

 [12] R.V. Padilla, G.Demirkaya, D.Y.Goswami, E.Stefanakos,M.M. Rahman, Heat transfer analysis of parabolic trough solar receiver, *App. Energy* **88** (2011) 5097–5110

[13].Fadar A E, Mimet A and García M P 2009 Modelling and performance study of a continuous adsorption refrigeration system driven by parabolic trough solar collector, *Solar Energy* **83** pp 850–61

[14] Montes MJ, Rovira A, Muñoz M and Martínez-Val J M  2011 Performance analysis of an Integrated Solar Combined Cycle using Direct Steam Generation in parabolic trough collectors, *App. Energy* **88** 3228–3238

[15] García I L,.Álvarez J L and Blanco D 2011 Performance model for parabolic trough solar thermal power plants with thermal storage, , *Solar Energy* **85** 2443–60

[16]  Barberena J G, Garcia, Sanchez M, Blanco M J , Lasheras C, Padrós A and Arraiza J 2011 Analysis of the influence of operational strategies in plant performance using SimulCET, simulation software for parabolic trough power plants,  *Solar Energy* **85** 721–735

 [17] Rolim M M, Fraidenraich F, and Tiba C 2009Analytic modeling of a solar power plant with parabolic linear collectors,  *Solar Energy* **83** 126–133

[18] Morin G,Dersch J, Platzer W , Eck M and Häberle A 2011 Comparison of Linear Fresnel and Parabolic Trough Collector power plants,  *Solar Energy* **84** 502-555

[19] Muñoz J and.Abánades A 2011 A technical note on application of internally finned tubes in solar parabolic trough absorber pipes, *Solar Energy* **85** 609–612

[20] Rojas M E, de Andrés M C and González L 2008 Designing capillary systems to enhance heat transfer in LS3 parabolic trough collectors for direct steam generation, *Solar Energy* **82** 53–60

[21] Al-Ansary and H, Zeitoun O  2011 Numerical study of conduction and convection heat losses from a half-insulated air-filled annulus of the receiver of a parabolic trough collector, *Solar Energy* **85** 3036–3045

[22] Petukhov B S and  Roizen L I 1964 Generalized relationships for heat transfer in a turbulent flow of gas in tubes of annular section. *High Temp* **2** 65–8.

[23] Kakac S , Shah RK and Aung W. Handbook of single-phase convective heat transfer. New York: John Wiley & Sons; 1987.

[24] Dushman S. Scientific foundations of vacuum technique. 2nd ed. New York: Wiley; 1962.

[25] T.H. Kuehn and R.J. Goldstein, A Parametric Study of Prandtl Number and Diameter Ratio Effects on Natural Convection Heat Transfer in Horizontal Cylindrical Annuli, J. Heat Transfer, Vol. 102, 768-770 (1980).

[26] Modest, M 2003Radiative heat transfer. 2nd ed. Burlington, MA: Academic Press;.

[27] Incropera F P 2006, Fundamentals of heat and mass transfer. 6th ed. Hoboken, NJ: Wiley

[28] Swinbank W. 1963, Long-wave radiation from clear skies. Quar J R Meteorol Soc;89 339–48.

[29] Duffie J A and Beckman WA 1980 Solar engineering of thermal processes. New York: Wiley

[30] Dudley V, Kolb G, Sloan M and Kearney D 1994 SEGS LS2 Solar Collector-Test Results. Report of Sandia National Laboratories.SAN94-1884.

[31]http://www.therminol.com/pages/bulletins/europe/therminol_vp1_anglais.pdf